Chemiluminescent fingerprints from airborne particulate matter: a luminol-based assay for the characterization of oxidative potential with kinetical implications

Pietro Morozzi[a]*, Luca Bolelli[b], Erika Brattich[c], Elida Nora Ferri[b], Stefano Girotti[b], Stefano Sangiorgi[b], J.A.G. Orza[d], Francisco Piñero-García[e,f], Laura Tositti[a]*

[a] Department of Chemistry "G. Ciamician", University of Bologna, Via Selmi, 2, 40126 Bologna, Italy

[b] Department of Pharmacy and Biotechnology, University of Bologna, Via S. Donato 15, 40127 Bologna, Italy

[c] Department of Physics and Astronomy, University of Bologna, Via Irnerio, 46, 40126 Bologna, Italy

[d] SCOLAb, Department of Applied Physics, University Miguel Hernandez de Elche, 03202, Elche, Spain

[e] Radiochemistry and Environmental Radiology Laboratory, Inorganic Chemical Department, Faculty of Sciences, University of Granada, 18077, Granada, Spain

[f] Department of Radiation Physics, Institute of Clinical Sciences, Sahlgrenska Academy, University of Gothenburg, Gula Stråket 2B, SE-413 45, Gothenburg, Sweden

***Corresponding authors:**

PhD student Pietro Morozzi; e-mail address: pietro.morozzi2@unibo.it; mailing address: Via Selmi 2, 40126 Bologna (ITALY).

Prof. Laura Tositti; e-mail address: laura.tositti@unibo.it; mailing address: Via Selmi 2, 40126 Bologna (ITALY).

ABSTRACT:

In this study, a new chemiluminescent method based on the dependence of luminol light emission induced by free radicals in airborne particulate matter (PM) is proposed as a screening assay for the rapid characterization of samples from different sources based on their redox properties. This parameter is considered critical for assessing particulate matter toxicity and its impacts on human health. We propose a cell-free, luminescent assay to evaluate the redox potential of particulate matter directly on the filters employed to collect it. A joint chemometric approach based on Principal Component Analysis and Hotelling Analysis was applied to quickly sort out ambient particulate samples with a significantly different light emission profile caused by Luminol reaction. Based on Spearman correlation analysis, the association of the samples light emission intensity with their chemical composition and emission sources was attempted.

The overall methodology was tested with certified reference materials and applied to two series of particulate matter samples previously subjected to thorough chemical speciation and subsequent source apportionment.

The results show the effectiveness of the luminescent method, allowing the quick assessment of particulate matter oxidative potential, but providing further evidence on the complexity of the oxidative potential determination in this kind of samples. The chemometric processing of the whole dataset clearly highlights the distinct behavior among the two series of samples, the certificate standard reference materials, and the blank controls, supporting the suitability of the approach.

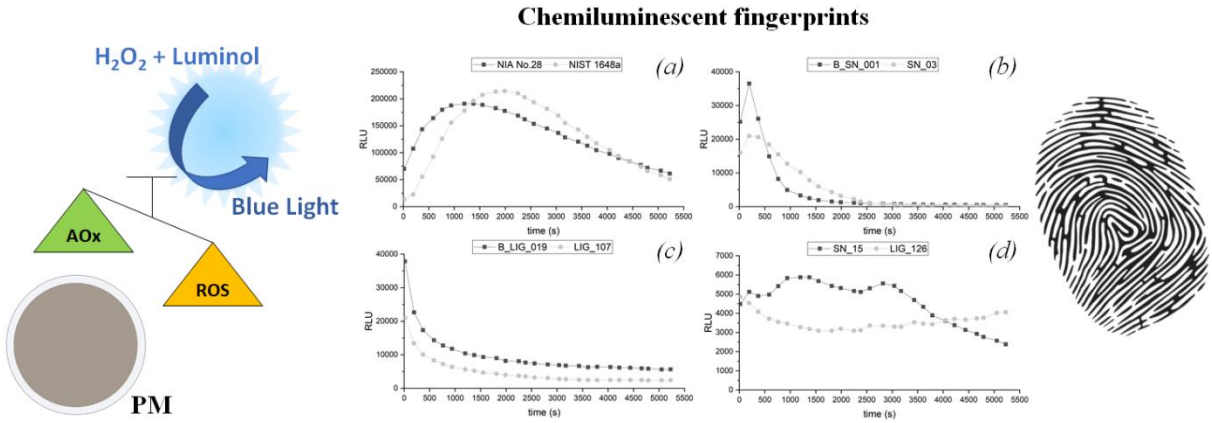

Keywords: *airborne particulate matter, oxidative potential, chemiluminescence, chemometrics, luminol*

HIGHLIGHTS

- Screening evaluation of particulate matter oxidative potential
- Luminol light emission over time as chemiluminescent fingerprint
- Relationship between the luminescence data and aerosol emission sources
- Effective discrimination of different particulate matter filters by Chemometrics

1. INTRODUCTION:

Airborne particulate matter (from now on PM) is one of the most serious and challenging pollutants to which the human population is exposed (Landrigan *et al.*, 2018). The health hazard from PM is historically recognized since ancient times (Claxton, 2014), though it is only in recent decades that the cause-effect relationships are being systematically investigated. To date, the outcomes of PM on human health account for a myriad of different diseases ranging from the lung-related ones to the cardiovascular (Cohen *et al.*, 2005; Pope III and Dockery, 2006; Rajagopalan *et al.* 2018), autoimmune (Zhao *et al.*, 2019), and non-communicable diseases (Schraufnagel *et al.*, 2019), which presently include diabetes, cognitive impairment, Alzheimer, and many others. For these reasons, environmental legislation is continuously evolving with regulations aiming to reduce the PM concentration within thresholds to minimize the risks to both the population and the environment. The main shreds of evidence are extensively collected from epidemiological inference (Pope III and Dockery, 2006; Shiraiwa *et al.*, 2017; Zhao *et al.*, 2019) and are accompanied by concurrent investigations aimed to associate the complex PM chemical composition with toxicity data and related health effects, proposing plausible mechanisms of cell-PM interactions.

Nowadays, the most accredited hypothesis is that health hazard from PM is due to a synergy between its chemical composition and size distribution of the particles, as well as that the potential damages depend both on exposure and dose, while a univocal mechanistic paradigm concerning what is triggering health effects in humans is not available yet, mainly due to the complexity of aerosol chemistry. In fact, PM chemical speciation continues to be challenging, reflecting source composition and complexity as well as the impacts of atmospheric recirculation and processing, which lead to the addition/formation of new pollutants over time.

PM mass load has been long recognized as the fundamental metric to assess aerosol environmental levels and inherent health risk in the range 20-50 $\mu g/m^3$ for PM_{10} (i.e., particles with an aerodynamic diameter smaller than or equal to 10 μm). However, some major components accounting for a large fraction of the PM mass load display relatively limited reactivity, such as

Secondary Inorganic Aerosol (SIA; ammonium, sulfates, and nitrates), sea salt, some of the mineral components, while organic and elemental carbon are associated with more critical compounds (Mauderly and Chow, 2008). PM hazard is mainly associated with trace elements and organic compounds involved in electron transfer processes though all these species are generally in concentration several orders of magnitude lower than the PM carrier mass load (Tositti, 2017; Kelly and Fussell, 2020; Pardo *et al.*, 2020). For example, EU air quality standards include regulations for PM_{10} and for a few of its chemical components such as Pb, Ni, Cd, As, BaP (i.e. benzo-a-pyrene) and assimilated PAHs (Polycyclic Aromatic Hydrocarbons) with concentration thresholds from the units up to hundreds of ng/m^3 (EU Directive 2008/50/EC), clearly showing the hazard derived from minor constituents rather than bulk PM concentration.

To date, there is a consensus that airborne particulate toxicity is mainly attributed to oxidative stress, the pathological condition originated from the breakdown of the physiological balance between the generation of Reactive Oxygen Species (ROS, including H_2O_2, $O_2^{\bullet-}$, $^1O_2$, $\cdot OH$, O_3, hypohalous acids, organic peroxides, …) and the antioxidant capacity of human tissues (see for example Janssen *et al.*, 2014; Riediker *et al.*, 2019; Pardo *et al.*, 2020). Non-neutralized free radicals lead to the damage of cells, tissues, and organs, as reported by Averill-Bates *et al.*, 2018.

Therefore, ROS concentration is considered as an efficient predictor of PM harmfulness and the term "oxidative potential" (OP), i.e., the ability to produce oxidative stress, has been consequently introduced as a suitable metric (Ayres *et al.*, 2008; Delfino *et al.*, 2013, and references therein).

Many different cell-free and cell-based methodologies have been proposed in the last decades for the evaluation of OP in PM, but so far no official standard method has been selected and accredited for routine use.

Cell-free assays, recently reviewed by Taylor Bates *et al.* (2019) and Pietrogrande *et al.* (2019), stand out for the assessment of PM's oxidative potential owing to their rapidity, limited costs, and the absence of highly specialized personnel compared to the cell-based analysis. They are ideal for analyzing the large number of PM filter samples collected on a routine basis by adopting different experimental approaches: the measurement of the depletion rate of natural antioxidants like ascorbic acid (AA) or glutathione (GSH); the measurement of the depletion rate of a chemical reductant like dithiothreitol (DTT); the measurement of the formation rate of ROS by Electronic Spin Resonance (ESR), High-Performance Liquid Chromatography or fluorescent probes.

These assays return different and even contrasting results due to the different sensitivity that each method shows with respect to the different redox-active compounds (Visentin *et al.*, 2016; Xiong *et al.*, 2017; Taylor Bates *et al.*, 2019). PM samples contain thousands of different chemicals, including several pro- and anti-oxidant, producing a net signal resulting from contrasting effects of

difficult interpretation. Moreover, the different experimental procedures employed in each method such as sampling procedure (Yang *et al.*, 2014), sample storage conditions (Fuller *et al.*, 2014), solvents used for the extraction (Verma *et al.*, 2012; Yang *et al.*, 2014; Calas *et al.*, 2017), extracting procedure (Miljevic *et al.*, 2014), or even reagent concentration (Lin and Zhen Yu, 2019) can lead to biased results.

In the attempt both to shed light on the factors affecting the assessment of PMs' OP and to find a rapid screening assay to characterize the different PMs, in this work we propose a new method for the assessment of OP based on the Total Oxidant Capacity determination by using the highly sensitive luminol (5-Amino-2,3-dihydrophthalazine-1,4-dione) chemiluminescent assay. This molecule is largely employed in various conditions to determine the amount of free radicals produced by a sample, the antioxidant power of different molecules and their amount, as well as the final balance of these two phenomena in the same matrix (Girotti *et al.*, 2000; Ferri *et al.*, 2006; Khan *et al.*, 2014).

Compared to other assays currently used in PM OP determination, which are mainly based on antioxidant molecules consumption, the luminol assay works completely different since it is based on its activation by oxidative reactions and then on the measurement of light emission intensity and kinetics (Agarwal *et al.*, 2004). Indeed, the analytical signal appears after its oxidation produced by free radicals, mainly H_2O_2 derived radicals, a reaction triggered by enzymes like peroxidases (Zhang *et al.*, 2018). PM was tested directly on the filters, cut to obtain various subsamples, without extraction procedures and analyzing many samples in short time on multiwall plates. Pragmatic and easy procedures of PM sample processing were selected while chemometric techniques, including multivariate and untargeted techniques, were extensively applied for the treatment of instrumental signals, data reduction, and classification.

2. MATERIALS AND METHODS:

2.1 Particulate matter and Certified PM Reference Materials samples

Two series of particulate matter samples, the SN and the LIG series, were collected on filters in Sierra Nevada (Spain) and in Liguria (NW Italy), respectively.

The Sierra Nevada sampling station, in southern Spain, is located at high altitude (2550 m a.s.l., 37.096 N, -3.387 W). The PM_{10} samples were collected in the framework of the FRESA Project (Impact of dust-laden African air masses and of stratospheric air masses in the Iberian Peninsula. Role of the Atlas Mountains, Ref: CGL2015-70741-R) on quartz filters (Ø 15 cm) by a high volume sampler, 30 m^3/h, (CAV-A/mb, MCV S.A., Spain) for a week (air volume sampled per filter = 5040

m^3). A total of 19 weekly filters were collected mainly during the summer period (from June to October 2016) and 3 field blank filters (i.e., filters that are taken to the field through the same procedure as samples, including transport to and from the sampling site, and storage in the field, and analysis, but are not used for collecting particulate matter, to ensure prevention of contamination of field samples), were processed.

The Liguria sampling station (NW Italy) is located in a narrow valley secluded by a complex mountainous topography with a small town, an industrial area with a large chemical plant and limited vehicular traffic. PM_{10} samples were collected on quartz filters (Ø 4.7 cm) by a HYDRA Dual Sampler, (Fai Instruments S.r.l., Italy), for 24 h at 2.3 m^3/h, (air volume sampled = 55.2 m^3). A total of 130 daily filters were collected from November 2014 to April 2015, plus 4 field blank filters.

Two standard reference materials of particulate matter were also analyzed: CRM No.28 Urban Aerosols by NIES (National Institute for Environmental Studies, Ibaraki Prefecture, Japan) and SRM 1648a - Urban Particulate Matter, by NIST (National Institute for Standards and Technology, MD, USA).

A home-made device was designed and assembled according to Fermo *et al.*, 2006 and Cuccia *et al.*, 2011 to collect the standards on filters. The system consists of a vacuum pump, a filter holder, plastic tubes for the connections, and a resuspension chamber. The system was carefully assembled to guarantee air-tightness. A scheme is shown in Figure 1.

The device allowed to obtain filters simulating typical PM samples based on known amounts of powdered reference materials determined by accurate weighing. The surface densities of the standards obtained were respectively 0.44 mg cm^{-2} for the NIES CRM No.28 and 0.34 mg cm^{-2} for the NIST SRM 1648a.

2.2 Chemical speciation and source apportionment of PM_{10}

Sierra Nevada (SN) and Ligurian (LIG) particulate matter samples were stored frozen in the dark at −10 °C and then subjected to an extensive chemical speciation as follows.

Shortly, the SN samples were analyzed by gravimetry to determine the PM_{10} mass (μg/m^3), by Ion Chromatography (IC) for the determination of the main water-soluble ions composition (EN 16913:2017), and by Particle Induced X-ray Emission (PIXE) for multielemental non-destructive analysis using the method already described in Lucarelli *et al.*, 2011 and Chiari *et al.*, 2018.

LIG samples have been subjected to the same analyses as those of SN, plus Inductively Coupled Plasma Mass Spectrometry (ICP-MS) determination of trace elements according to EN 14902:2005, IC determination of anhydrous sugars (Piazzalunga *et al.*, 2010), Thermal-optical analysis (TOA) for elemental carbon (EC) and organic carbon (OC) assessment (Piazzalunga *et al.*,

2011), and Gas Chromatography-Mass Spectrometry (GC-MS) for the determination of Polycyclic Aromatic Hydrocarbons (PAHs) (EPA 1998, EPA 2007).

A receptor modelling for Source Apportionment (SA) was applied in order to derive information about their sources and their contribution to PM levels (Belis *et al.*, 2019).

Owing to the limited number of samples available, source apportionment of SN samples (19 sample x 19 variables) was performed by means of the Chemical Mass Balance (CMB) approach, using the EPA-CMB 8.2 software (EPA, 2004). Suitable source profiles were selected from the European data base for PM source profiles (Pernigotti *et al.*, 2016). After several runs, the final CMB solution was chosen on the basis of its best statistical performance indexes, i.e. R-square (R^2; target = 0.8-1.0), Chi-square (χ^2; target = 0-4), and calculated-to-measured ratios for the chemical species used (C/M: target = 0.5-2.0).

Source Apportionment of LIG samples (129 sample x 42 variables) was performed by Positive Matrix Factorization (PMF) (Paatero and Tapper, 1993), a multivariate factor analysis technique which uses experimental uncertainty for scaling matrix elements and constrains factor elements to be non-negative. This analysis employed the EPA PMF5.0 software (Norris *et al.*, 2014).

2.3 Chemiluminescent assay

Chemiluminescence reagents were all from the WesternSure® PREMIUM kit (LI-COR, Lincoln, NE, USA).

The chemiluminescent assay was carried out on environmental samples, blanks, and standard samples using 96-well plates (8 x 12 well strips). Quartz filter punches (Ø = 8 mm) were obtained by die-cutting quartz membranes. Each punch was carefully transferred face-up to the bottom of each well directly from the die-cutting tool. 100 µl of the mixture (1:1) of solution A (containing luminol and enhancer) and solution B (fresh H_2O_2 solution) were added to each well of the plate using a multichannel pipette. Immediately after the reagent addition, the light emission intensity was measured using a VICTOR Light microplate luminometer and expressed as Relative Luminescence Units (RLU) . The luminometer recorded sequentially the light emitted in one second by each well, taking 124 s to read the whole plate. The chemiluminescence values were recorded for about 1 hour (28 values), obtaining a light emission profile (RLU vs. Time, in seconds). The precision of the measurements was quantified as the relative standard deviation of a set of replicates, computed from the analysis of six punches of a single filter, chosen to the scope. The result was about 11% and included the PM filter anisotropy, i.e. the not homogeneous distribution of the particulate materials on the filter, which cannot be precisely the same in every point of the filter.

2.4 Chemometrics

The experimental dataset was extensively processed by chemometric tools for a) data classification and reduction, and b) for correlation.

After suitable data standardization by subtracting the column-average from every element in the column (i.e. centering, van den Berg *et al.*, 2006), Principal Components Analysis (PCA) (Bro and Smilde, 2014) and Hotelling analysis were applied to the whole dataset including chemiluminescence data using The Unscrambler V. 10.4 (Camo, Oslo, Norway).

PCA and Hotelling analyses were computed at a confidence level of 95% (Jolliffe, 2005). While PCA allowed to identify sample groupings, Hotelling analysis provides a geometrical representation of PCA scores relatively to an ellipsoid. The samples outside the ellipsoid are considered significantly different from those inside it (at the confidence level of 95%) therefore highlighting distinct sample behavior in terms of OP and composition.

A Spearman correlation analysis between emission source contributions and OP data, defined as the integrals of luminol light emission over the acquisition time, was performed for each a priori class (Wissler, 1905). Spearman analysis is a more appropriate measure of association than Pearson's for describing the monotonic relationship between two variables instead of a linear relationship and, therefore, best suited in this case study (Schober *et al.*, 2018).

Before the correlation analysis, all OP data were normalized by filter surface and volume of sampled air in order to provide dimensional consistency and homogeneity with the source contributions deduced by source apportionments, expressed as µg in the whole filter per m^3 of sampled air. In this way, an OP value was defined as the chemiluminescence (from now on, CL) value of the whole filter on m^3 of sampled air (RLU/m^3).

The Spearman correlation analyses were carried out by the software OriginPro 2018 (OriginLab, Northampton, USA).

3. RESULTS AND DISCUSSION:

3.1 The chemiluminescent assay: analysis of the chemiluminescence profile

CL luminol assays are based on instrumental data representing the light emission intensity over time. The kinetics of the luminol oxidation, which leads to an excited intermediate and then to its decay to a stable final product accompanied by light emission, can be completely different in the various experimental conditions since the reaction mechanism is quite complicated, as shown in Rose and Waite, 2001.

It depends on the reagents' ratio in the sample, on the rate and/or chemical nature of radicals production, on the presence of enhancers or scavenging molecules which can be consumed or produced during the reaction. Their simultaneous presence will result in a signal dependent on their balanced effects. Owing to PM complexity, we firstly examined the spectral output obtained, in order to define the best instrumental conditions to apply and to identify possible, characterizing differences among the samples. The trend of the light emission values vs. time clearly showed different kinetic patterns in luminol oxidation and, consequently, in ROS production rate or in oxidant/antioxidant capacity balance. The luminescence emission intensity vs. time trends can be basically classified according to diagrams depicted in Figure 2.

The differences in the luminescence kinetics are plausibly associated with the chemical complexity and unicity of each individual PM sample and with the consequent relative stability and balance of the free radicals production-scavenging phenomena (Squadrito *et al.*, 2001; Dellinger *et al.*, 2007; Feld-Cook *et al.*, 2017; Tong *et al.*, 2018). The emission profile is implicitly informative of the nature and half-life of the ROS active species originated in the collected PM, as well as of the interactions between them and other components, information that can be used as a proxy of the particulate oxidative potential. The attempt to identify this intriguing connection between the chemical composition and the reactive species highlighted by the chemiluminescent reaction was the basic challenge to justify the application of this method. Our observation shows clearly how source profiles affect PM composition and the associated availability of redox active species, each one with its specific properties, including solubilization in the liquid medium (possibly critical for elements like the Fe(II)/Fe(III) couple, to which luminol is extremely sensitive by the way) (Khan *et al.*, 2014). With the exception of samples with a flat CL profile, the major differences are observed at the beginning of the emission profile when maximum intensity is reached with very variable rates, after which these samples reveal an asymptotic relaxation of CL. It is to note how the certified reference materials (CRMs) used to check the procedure performance are particularly slow in CL development (up to tenths of minutes as compared to hundreds of seconds for our samples) possibly indicating not only different PM composition and source profile mixtures, but possibly aging of CRMs and/or an influence of handling procedures and inherent environmental/atmospheric redox conditions.

Our findings show quite clearly that in the conditions observed the choice of a maximum for OP assessment is extremely arbitrary. For this reason, on account of metrologic requisites, we decided to use the integral of RLU over the 0-5000 seconds time interval as the spectral parameter on which quantifying the differences in the PM redox behavior.

3.2 Chemometric analyses

3.2.1 Comprehensive PCA and evaluation of luminol chemiluminescence as a proxy for PM Oxidation Potential

The calculation of the Principal Components (PCs) of a given dataset allowed identifying groups of variables with similar and coherent behavior as compared to the other groups. In this case the discriminating parameter is the "chemiluminescent fingerprints" linking their oxidative potentials to their composition.

As shown in the scores plot reported in Figure 3, PC-1 and PC-2 together covered almost the entire explained variance (≈ 100%), which means an exceptionally high capability to describe the initial dataset. High discrimination between NIA No.28, NIST 1648a, as compared to all the other analyzed samples, is observed**.** Good discrimination between LIG and SN samples is found (except for some LIG samples). Even the respective blanks are well separated from each other. The LIG blanks are entirely resolved from the LIG samples, while the SN blanks are slightly overlapped to the SN samples.

These results reveal that the CL profiles are significant, and can be therefore taken as meaningful measurements of OPs in connection with their respective composition and redox properties and, therefore, of a given receptor site.

3.2.2 Class-PCA and Hotelling analysis

Two different class-PCA were performed and the relative scores plots are reported in Figure 4 (a, LIG samples) and (b, SN samples). Hotelling analysis calculates an ellipsoid for the PCA scores plot. The samples outside such ellipsoid are considered significantly different from those inside of it (at the confidence level of 95%) and therefore are highlighted as samples with significantly different OP is with respect to all the others.

The Hotelling ellipses at the 95% confidence level were computed and displayed in both scores plots. This method allows to distinguish the samples with significantly different CL profile though within the same group.

In both cases, the explained variance is very high for the first two principal components (PC-1 + PC-2): respectively 98% for LIG class-PCA and 95% for SN class-PCA. This confirms the representativeness of the starting dataset.

In Figure 4 (a), almost all the samples are enclosed within the Hotelling ellipse: only nine LIG samples appeared to be significantly different, possibly in connection with the seasonal variation in atmospheric circulation leading to a higher degree of data scattering. These samples were collected

during the cold season characterized by a different circulation pattern as compared to the warm season and being, therefore, affected by distinct emissive profiles.

On the contrary, the Sierra Nevada samples were highly coherent, being all sampled during a single season.

3.3 Source Apportionment of the PM samples

In order to associate statistically the OPs based on luminol CL with the chemical fingerprints of the emission sources of PM_{10} in the location studied, in this paragraph we describe the results of receptor modeling obtained at the two locations herein investigated.

3.3.1 Sources of SN samples

As previously described, the SN dataset includes a small number of weekly samples (19) not suitable for the use of PMF which is a comparatively more frequently used approach in source apportionment (Belis *et al.*, 2019). The best solution of the Chemical Mass Balance (CMB) for the source apportionment of Sierra Nevada (SN) samples was achieved by the selection of four SPECIEUROPE (Pernigotti *et al.*, 2016) source profiles: 17 - Soil Dust Composite Rural (cr), 157 - Aged sea spray (ss), 288 - Nitrate_PMF5 (nt), and 291 – Sulphate (sp). The PM_{10} fraction of reconstructed mass (%) is 85 % and the results are in agreement with the PM mass reconstruction based on empirical equations performed on the basis of chemical speciation data (see for example Chow *et al.*, 2015).

Soil Dust Composite Rural basically captures the Saharan dust incursion events typical of high-altitude locations across the Mediterranean region (Riccio *et al.*, 2009; Cusack *et al.*, 2012; Israelevich *et al.*, 2012; Tositti *et al.*, 2014; Brattich *et al.*, 2015; Cabello *et al.*, 2016; Cuevas *et al.*, 2017) representing most of the mass of the PM_{10} (about 75%). Secondary Inorganic Aerosol (SIA; ammonium, sulfates, and nitrates) derives from the gas-to-particle conversion from SO_2 and NO_x in the atmosphere (Schaap *et al.*, 2004; Pathak *et al.*, 2009). These sources contribute respectively to 5% and 3% of the PM_{10} at SN. The Aged sea spray source contributes 2% to PM_{10} mass, mainly constituted of sodium chloride (NaCl), which undergoes atmospheric aging processes due to their long-range atmospheric transport. The pie chart representing the contribution of the four sources to PM_{10} mass is reported in Figure 5.

3.3.2 Sources of LIG samples

PMF model requires an accurate and detailed knowledge in terms of number of observed data and of chemical parameters across the studied area in order to capture a reliable quantitative source

363 profile. A six-factor solution was selected as the best result on the basis of the fitting parameters, the
364 convergence of calculated Q to the expected value, a parameter estimating the goodness of the fit and
365 the distribution of residuals (Brown *et al.*, 2015). The six factors obtained are: secondary nitrate,
366 biomass burning, industrial emissions, road dust, fuel oil burning, and sea salt. The comparison
367 between measured (input data) and modeled values together with the distribution of residuals was
368 evaluated, indicating a good model performance in reconstructing PM_{10}, with a coefficient of
369 determination equal to 0.96 and accounting for 80% of the total PM mass. The Factor Fingerprints
370 screen is reported in Fig. 6.
371 The secondary nitrate source (23.7%) includes all the high-temperature active sources, e.g.
372 biomass combustion, the industrial settlement, and traffic. The biomass burning source (24.7%) is
373 mainly due to wood burning during the winter period. The industrial high temperature facility
374 emissive contribution covers about 17.1% of the PM_{10} at the receptor site contributing however
375 substantially to OC, EC, and sulfates beside nitrates. Road dust (11.7%) comprises mainly coarse
376 mineral particles from friction and wear of the mechanic components such as brakes, tires, and asphalt
377 including trace elements of potential toxicological relevance, e.g. Ni and others. Fuel oil burning
378 (16.7%) identifies the combustion of heavy oils due to trucks, diesel, and marine traffic. The sea salt
379 source (6.1%) has the typical "marine aerosol" imprint.
380
381 *3.4 Spearman correlation analysis*
382 For each class (SN and LIG samples), a Spearman correlation analysis between source
383 contributions data from CMB (SN samples) or PMF (Ligurian samples) and the OPs was computed;
384 the obtained correlation coefficients are reported in Table 1.
385 Concerning SN samples, all the emission sources were significantly and positively correlated
386 with the light emission intensity. Therefore, all these emission sources contribute significantly to the
387 increase of free radicals in these samples, i.e. to the particulate material's oxidative potential. It is
388 interesting to note how the mineral dust source (cr) does not show the highest correlation, despite its
389 high weight contribution (75% of the total PM_{10}).
390 The results for the LIG samples were completely different: OP is negatively correlated with
391 biomass burning emission source, which quantitatively is one of the most relevant emission sources
392 (14.7% of the total PM_{10}) while the other emission sources were not significantly correlated with the
393 oxidative potential. The absence of significant correlations with other emission sources may be
394 related to the sampling period of the Ligurian filters (from November 2014 to April 2015), which are
395 mainly in the cold season and, therefore, with a significant contribution of biomass burning sensibly
396 affecting oxidative potential with respect to other sources. Correlation analysis on a semi-seasonal

basis indicates how the biomass burning component is more negatively correlated with the oxidative potential in the coldest months of the sampling campaign (rs =-0.83) and then decreases the negative correlation moving towards the hot season (rs =-0.51).

Despite the statistical significance of LIG results, this anticorrelation has drawn our attention since it has been widely demonstrated how combustion PM led to an increase *in vivo* of oxidative damages (Lighty *et al.*, 2000; Mauderly and Chow, 2008).

One plausible explanation is that Biomass Burning components in PM operate free radical scavenging activity mechanism, neutralizing many of the radical species during the chemiluminescence assay.

As previously reported for LIG class in Figure 4(a), 9 samples behaved significantly different from the others.

Figure 7 represents the boxplots of the oxidative potential and biomass burning components for the samples inside the 95%-Hotelling ellipses and for the samples outside the latter, respectively.

As shown in Figure 7, the 9 LIG samples outside the Hotelling ellipse were characterized by higher light emission and lower Biomass Burning component compared to the other 120 samples. In particular, the higher emission of these specific samples seems due to the lower biomass burning component, as evidenced by the significant negative correlation seen above. This could be in agreement with seasonality, as these filters were sampled in the hot season characterized by less heating through wood combustion. The color of the filters, less dark than the others, also supports this hypothesis suggesting the presence of a smaller amount of biomass burning components.

Therefore, the 9 LIG samples highlighted by the screening method proposed in this paper turn out to be those with the lower biomass burning components, those with higher light intensity from oxidized luminol and with the lighter color of the filters.

4. CONCLUSIONS:

In this article, a new chemiluminescence method based on the sensitivity of luminol to radicals is proposed for particulate matter samples rapid characterization.

This method allows to simultaneously analyses up to 96 PM filter portions without any chemical sample pre-treatment (no liquid extraction) and in a short time (approximately 1 hour). The cost of this kind of analysis, estimated as the ratio between the price of the used reagents and the number of tests that can be carried out with them, is around 50 cents per sample. All these advantages make this technique a screening one, which can also be performed by non-highly specialized personnel.

The primary purpose of this methodology is the rapid identification of PM samples that significantly differ from all others as regards their composition. Subsequently, it is necessary to understand why these samples behave differently, through a comparison of chemiluminescence values with the chemical-physical characterization data or, even better, information on their emission sources.

Two different series of samples were used for the technique validation, well characterized on their emission sources through the application of Source Apportionment techniques: Sierra Nevada (S-Spain) samples, which contain mainly mineral dust from North Africa, and Ligurian (NW-Italy) samples, composed mainly by organic compounds deriving from biomass burning and industrial combustions.

The chemiluminescence signals obtained from this method are profiles of light emission over time dependent on free radicals amount resulting from the balance between the radical producing components and the radicals trapping ones, i.e. from the PM chemical composition. This emission kinetics showed different shapes and represented the final result of all chemical phenomena occurring in that specific, and complex, mixture each PM sample is made of. Indirectly, the light intensity indicated the OP of each sample in terms of the amount of active free radicals.

These light emission profiles were interpreted and considered holistically for the application of non-targeted chemometric techniques which allowed the identification of distinct samples. Subsequently, Spearman's correlation analysis allowed to determine the relationship between luminescence and emission source contributions, specifically linking the PM filters selected by the screening method as samples attributed to a well-defined source of emission.

This screening method did not identify any Sierra Nevada sample with chemiluminescence profile significantly different from the other ones of this set, while 9 Ligurian samples significantly different were identified. The latter have a higher light emission, and therefore a higher oxidative potential, associated with a lower presence of the Biomass Burning component on these filters. Although this, clearly demonstrated, correlation could seem contradictory to a first sight, it can be simply explained by the specific mechanism of luminol emission, which reveals both the pro- and antioxidant components at the same time.

Based on what was previously reported, the effectiveness of the proposed screening technique was proven, and this means that this method can join the others analytical techniques used for PM OP assessment already reported in the scientific literature.

ACKNOWLEDGEMENTS:

We are greatful to prof. María Ángeles Ferro García and Abel Milena Pérez in the Radiochemistry and Environmental Radiology Laboratory of the Inorganic Chemistry Department of University of Granada (LABRADIQ) for kindly providing the Sierra Nevada (SN) samples used in this work. Heartfelt thanks to Josep Mestres Sanna and Adrià Simon Ortiz for the assistance in the experimental activity.

FUNDING:

This work was funded by Fundamental Oriented Research (RFO) 2018-2019 and 2019-2020, University of Bologna (Italy).

REFERENCES:

Agarwal, A., S R Allamaneni, S., & M Said, T. (2004). Chemiluminescence technique for measuring reactive oxygen species. *Reproductive Biomedicine Online*, *9*, 466–468. https://doi.org/10.1016/S1472-6483(10)61284-9

Averill-Bates, D., Chow-shi-yée, M., Grondin, M., & Ouellet, F. (2018). Activation of apoptosis signaling pathways by reactive oxygen species. *Cryobiology*, *80*, 170. https://doi.org/10.1016/j.cryobiol.2017.10.064

Ayres, J. G., Borm, P., Cassee, F. R., Castranova, V., Donaldson, K., Ghio, A., Harrison, R. M., Hider, R., Kelly, F., & Kooter, I. M. (2008). Evaluating the toxicity of airborne particulate matter and nanoparticles by measuring oxidative stress potential—a workshop report and consensus statement. *Inhalation Toxicology*, *20*(1), 75–99.

Belis, C., Favez, O., Mircea, M., Diapouli, E., Manousakas, M.-I., Vratolis, S., Gilardoni, S., Paglione, M., Močnik, G., Mooibroek, D., Takahama, S., Vecchi, R., Paatero, P., Salvador, P., & Decesari, S. (2019). *European guide on air pollution source apportionment with receptor models - Revised version 2019.* https://doi.org/10.2760/439106

Brattich, E, Hernández-Ceballos, M. A., Cinelli, G., & Tositti, L. (2015). Analysis of 210Pb peak values at Mt. Cimone (1998–2011). *Atmospheric Environment*, *112*, 136–147. https://doi.org/https://doi.org/10.1016/j.atmosenv.2015.04.020

Brattich, Erika, Riccio, A., Tositti, L., Cristofanelli, P., & Bonasoni, P. (2015). An outstanding Saharan dust event at Mt. Cimone (2165 m asl, Italy) in March 2004. *Atmospheric Environment*, *113*, 223–235.

Bro, R., & Smilde, A. (2014). Principal component analysis. *Analytical Methods*, *6*, 2812. https://doi.org/10.1039/c3ay41907j

Brown, S. G., Eberly, S., Paatero, P., & Norris, G. A. (2015). Methods for estimating uncertainty in PMF solutions: Examples with ambient air and water quality data and guidance on reporting PMF results. *Science of the Total Environment*, *518*, 626–635.

Cabello, M., G. Orza, J., Dueñas, C., Liger, E., Gordo, E., & Cañete, S. (2016). Back-trajectory analysis of African dust outbreaks at a coastal city in southern Spain: Selection of starting heights and assessment of African and concurrent Mediterranean contributions. *Atmospheric Environment*, *140*. https://doi.org/10.1016/j.atmosenv.2016.05.047

Calas, A., Uzu, G., Martins, J., Voisin, D., Spadini, L., Lacroix, T., & Jaffrezo, J.-L. (2017). The importance of simulated lung fluid (SLF) extractions for a more relevant evaluation of the oxidative potential of particulate matter. *Scientific Reports*, *7*. https://doi.org/10.1038/s41598-017-11979-3

Chiari, M., Yubero, E., Calzolai, G., Lucarelli, F., Crespo, J., Galindo, N., Nicolás, J. F., Giannoni, M., & Nava, S. (2018). Comparison of PIXE and XRF analysis of airborne particulate matter samples collected on Teflon and quartz fibre filters. *Nuclear Instruments and Methods in Physics Research Section B: Beam Interactions with Materials and Atoms*, *417*, 128–132. https://doi.org/https://doi.org/10.1016/j.nimb.2017.07.031

Chow, J. C., Lowenthal, D. H., Chen, L.-W. A., Wang, X., & Watson, J. G. (2015). Mass reconstruction methods for PM2.5: a review. *Air Quality, Atmosphere & Health*, *8*(3), 243–263. https://doi.org/10.1007/s11869-015-0338-3

Claxton, L. D. (2014). The history, genotoxicity, and carcinogenicity of carbon-based fuels and their emissions. Part 2: solid fuels. *Mutation Research/Reviews in Mutation Research*, *762*, 108-122.

Cuccia, E., Piazzalunga, A., Bernardoni, V., Brambilla, L., Fermo, P., Massabò, D., Molteni, U., Prati, P., Valli, G., & Vecchi, R. (2011). Carbonate measurements in PM10 near the marble quarries of Carrara (Italy) by infrared spectroscopy (FT-IR) and source apportionment by positive matrix factorization (PMF). *Atmospheric Environment*, *45*(35), 6481–6487.

Cuevas, E., Gómez-Peláez, A. J., Rodríguez, S., Terradellas, E., Basart, S., García, R. D., García, O. E., & Alonso-Pérez, S. (2017). The pulsating nature of large-scale Saharan dust transport as a result of interplays between mid-latitude Rossby waves and the North African Dipole Intensity. *Atmospheric Environment*, *167*, 586–602.

Cusack, M., Alastuey, A., Pérez, N., Pey, J., & Querol, X. (2012). Trends of particulate matter (PM2. 5) and chemical composition at a regional background site in the Western Mediterranean over the last nine years (2002–2010). *Atmos. Chem. Phys*, *12*(18), 8341–8357.

Delfino, R. J., Staimer, N., Tjoa, T., Gillen, D. L., Schauer, J. J., & Shafer, M. M. (2013). Airway inflammation and oxidative potential of air pollutant particles in a pediatric asthma panel. *Journal of Exposure Science & Environmental Epidemiology*, *23*(5), 466–473.

Dellinger, B., Lomnicki, S., Khachatryan, L., Maskos, Z., Hall, R. W., Adounkpe, J., McFerrin, C., & Truong, H. (2007). Formation and stabilization of persistent free radicals. *Proceedings of the Combustion Institute*, *31*(1), 521–528.

EN 14902:2005. Ambient air quality - Standard method for the measurement of Pb, Cd, As and Ni in the PM10 fraction of suspended particulate matter.

EN 16913:2017. Ambient air - Standard method for measurement of $NO3^-$, $SO4^{2-}$, Cl^-, NH_4^+, Na^+, K^+, Mg^{2+}, Ca^{2+} in PM2,5 as deposited on filters.

EPA. 1998. "Method 8270D (SW-846): Semivolatile Organic Compounds by Gas Chromatography/ Mass Spectrometry (GC/MS)," Revision 4. www.epa.gov

EPA. 2004. "EPA-CMB8.2 User's Manual". www.epa.gov

EPA. 2007. "Method 3550C (SW-846): Ultrasonic Extraction". www.epa.gov

EU Directive 2008/50/EC (2008). Directive 2008/50/EC of the European Parliament and of the Council of 21 May 2008 on ambient air quality and cleaner air for Europe. *Official Journal of the European Union*.

Feld-Cook, E. E., Bovenkamp-Langlois, L., & Lomnicki, S. M. (2017). Effect of particulate matter mineral composition on environmentally persistent free radical (EPFR) formation. *Environmental Science & Technology*, *51*(18), 10396–10402.

Fermo, P., Piazzalunga, A., Vecchi, R., Valli, G., & Ceriani, M. (2006). A TGA/FT-IR study for measuring OC and EC in aerosol samples. *Atmospheric Chemistry and Physics*, *6*(1), 255-266.

Ferri, E., Girotti, S., Cerretani, L., Bendini, A. (2006). Various luminescent methods applied to evaluate olive oil Total Antioxidant Capacity. *Luminescence*, *21*(6), 358-359

Fuller, S. J., Wragg, F. P. H., Nutter, J., & Kalberer, M. (2014). Comparison of on-line and off-line methods to quantify reactive oxygen species (ROS) in atmospheric aerosols. *Atmospheric Environment*, *92*, 97–103. https://doi.org/10.1016/j.atmosenv.2014.04.006

Girotti, S., Fini, F., Ferri, E., Budini, R., Piazzi, S., & Cantagalli, D. (2000). Determination of superoxide dismutase in erythrocytes by a chemiluminescent assay. *Talanta*, *51*(4), 685–692.

Israelevich, P., Ganor, E., Alpert, P., Kishcha, P., & Stupp, A. (2012). Predominant transport paths of Saharan dust over the Mediterranean Sea to Europe. *Journal of Geophysical Research: Atmospheres*, *117*(D2).

Janssen, N. A. H., Yang, A., Strak, M., Steenhof, M., Hellack, B., Gerlofs-Nijland, M. E., Kuhlbusch, T., Kelly, F., Harrison, R., & Brunekreef, B. (2014). Oxidative potential of particulate matter collected at sites with different source characteristics. *Science of the Total Environment*, *472*, 572–581.

Jolliffe, I. (2005). Principal component analysis. 2nd ed. *Http://Lst-Iiep.Iiep-Unesco.Org/Cgi-Bin/Wwwi32.Exe/[In=epidoc1.in]/?T2000=017716/(100)*, *98*. https://doi.org/10.1002/0470013192.bsa501

Kelly, F. J., & Fussell, J. C. (2020). Toxicity of airborne particles—established evidence, knowledge gaps and emerging areas of importance. *Philosophical Transactions of the Royal Society A: Mathematical, Physical and Engineering Sciences*, *378*(2183), 20190322. https://doi.org/10.1098/rsta.2019.0322

Khan, P., Idrees, D., Moxley, M. A., Corbett, J. A., Ahmad, F., von Figura, G., Sly, W. S., Waheed, A., & Hassan, M. I. (2014). Luminol-based chemiluminescent signals: clinical and non-clinical application and future uses. *Applied Biochemistry and Biotechnology*, *173*(2), 333–355. https://doi.org/10.1007/s12010-014-0850-1

Landrigan, P. J., Fuller, R., Acosta, N. J. R., Adeyi, O., Arnold, R., Baldé, A. B., Bertollini, R., Bose-O'Reilly, S., Boufford, J. I., & Breysse, P. N. (2018). The Lancet Commission on pollution and health. *The Lancet*, *391*(10119), 462–512.

Lighty, J., Veranth, J., & Sarofim, A. (2000). Combustion Aerosols: Factors Governing Their Size and Composition and Implications to Human Health. *Journal of the Air & Waste Management Association (1995)*, *50*, 1565–1618; discussion 1619. https://doi.org/10.1080/10473289.2000.10464197

Lin, M., & Zhen Yu, J. (2019). Dithiothreitol (DTT) concentration effect and its implications on the applicability of DTT assay to evaluate the oxidative potential of atmospheric aerosol samples. *Environmental Pollution*, *251*. https://doi.org/10.1016/j.envpol.2019.05.074

Lucarelli, F., Nava, S., Calzolai, G., Chiari, M., Udisti, R., & Marino, F. (2011). Is PIXE still a useful technique for the analysis of atmospheric aerosols? The LABEC experience. *X-Ray Spectrometry*, *40*, 162–167. https://doi.org/10.1002/xrs.1312

Mauderly, J. L., & Chow, J. C. (2008). Health Effects of Organic Aerosols. *Inhalation Toxicology*, *20*(3), 257–288. https://doi.org/10.1080/08958370701866008

Miljevic, B., Hedayat, F., Stevanovic, S., E. Fairfull-Smith, K., Bottle, S., & Ristovski, Z. (2014). To Sonicate or Not to Sonicate PM Filters: Reactive Oxygen Species Generation Upon Ultrasonic Irradiation. *Aerosol Science and Technology*, *48*. https://doi.org/10.1080/02786826.2014.981330

Norris, G., Duvall, R., Brown, S., & Bai, S. (2014). *EPA Positive Matrix Factorization (PMF) 5.0 Fundamentals and User Guide*. www.epa.gov

Paatero, P., & Tapper, U. (1993). Analysis of different modes of factor analysis as least squares fit problems. *Chemometrics and Intelligent Laboratory Systems*, *18*(2), 183–194. https://doi.org/https://doi.org/10.1016/0169-7439(93)80055-M

Pardo, M., Qiu, X., Zimmermann, R., & Rudich, Y. (2020). Particulate Matter Toxicity Is Nrf2 and Mitochondria Dependent: The Roles of Metals and Polycyclic Aromatic Hydrocarbons. *Chemical Research in Toxicology*, *33*(5), 1110–1120. https://doi.org/10.1021/acs.chemrestox.0c00007

Pathak, R. K., Wu, W. S., & Wang, T. (2009). Summertime $PM_{2.5}$ ionic species in four major cities of China: nitrate formation in an ammonia-deficient atmosphere. *Atmos. Chem. Phys.*, *9*(5), 1711–1722. https://doi.org/10.5194/acp-9-1711-2009

Pernigotti, D., Belis, C. A., & Spano, L. (2016). SPECIEUROPE: The European data base for PM source profiles. *Atmospheric Pollution Research*, *7*(2), 307–314.

Piazzalunga, A, Bernardoni, V., Fermo, P., Valli, G., & Vecchi, R. (2011). On the effect of water-soluble compounds removal on EC quantification by TOT analysis in aerosol samples. *Atmospheric Chemistry & Physics Discussions*, *11*(7).

Piazzalunga, Andrea, Fermo, P., Bernardoni, V., Vecchi, R., Valli, G., & de Gregorio, M. A. (2010). A simplified method for levoglucosan quantification in wintertime atmospheric particulate matter by high performance anion-exchange chromatography coupled with pulsed amperometric detection. *International Journal of Environmental Analytical Chemistry*, *90*(12), 934–947. https://doi.org/10.1080/03067310903023619

Pietrogrande, M. C., Russo, M., & Zagatti, E. (2019). Review of PM Oxidative Potential Measured with Acellular Assays in Urban and Rural Sites across Italy. *Atmosphere*, *10*(10). https://doi.org/10.3390/atmos10100626

Pope III, C. A., & Dockery, D. W. (2006). Health effects of fine particulate air pollution: lines that connect. *Journal of the Air & Waste Management Association*, *56*(6), 709–742.

Riccio, A., Chianese, E., Tositti, L., Baldacci, D., & Sandrini, S. (2009). Modeling the transport of Saharan dust toward the Mediterranean region: an important issue for its ecological implications. *Ecological Questions*, *11*, 65–72.

Riediker, M., Zink, D., Kreyling, W., Oberdörster, G., Elder, A., Graham, U., Lynch, I., Duschl, A., Ichihara, G., Ichihara, S., Kobayashi, T., Hisanaga, N., Umezawa, M., Cheng, T.-J., Handy, R., Gulumian, M., Tinkle, S., & Cassee, F. (2019). Particle toxicology and health - where are we? *Particle and Fibre Toxicology*, *16*(1), 19. https://doi.org/10.1186/s12989-019-0302-8

Rose, A. L., & Waite, T. D. (2001). Chemiluminescence of Luminol in the Presence of Iron(II) and Oxygen: Oxidation Mechanism and Implications for Its Analytical Use. *Analytical Chemistry*, *73*(24), 5909–5920. https://doi.org/10.1021/ac015547q

Schaap, M., van Loon, M., ten Brink, H. M., Dentener, F. J., & Builtjes, P. J. H. (2004). Secondary inorganic aerosol simulations for Europe with special attention to nitrate. *Atmos. Chem. Phys.*, *4*(3), 857–874. https://doi.org/10.5194/acp-4-857-2004

Schober, P., Boer, C., & Schwarte, L. A. (2018). Correlation Coefficients: Appropriate Use and Interpretation. *Anesthesia & Analgesia*, *126*(5). https://journals.lww.com/anesthesia-analgesia/Fulltext/2018/05000/Correlation_Coefficients__Appropriate_Use_and.50.aspx

Shiraiwa, M., Ueda, K., Pozzer, A., Lammel, G., Kampf, C. J., Fushimi, A., Enami, S., Arangio, A. M., Fröhlich-Nowoisky, J., & Fujitani, Y. (2017). Aerosol health effects from molecular to global scales. *Environmental Science & Technology*, *51*(23), 13545–13567.

642 Squadrito, G. L., Cueto, R., Dellinger, B., & Pryor, W. A. (2001). Quinoid redox cycling as a
643 mechanism for sustained free radical generation by inhaled airborne particulate matter. *Free Radical*
644 *Biology and Medicine*, *31*(9), 1132–1138.

645 Taylor Bates, J., Fang, T., Verma, V., Zeng, L., Weber, R., E Tolbert, P., Y Abrams, J., Sarnat, S.,
646 Klein, M., Mulholland, J., & Russell, A. (2019). Review of Acellular Assays of Ambient Particulate
647 Matter Oxidative Potential: Methods and Relationships with Composition, Sources, and Health
648 Effects. *Environmental Science & Technology*, *53*. https://doi.org/10.1021/acs.est.8b03430

649 Tong, H., Lakey, P. S. J., Arangio, A. M., Socorro, J., Shen, F., Lucas, K., Brune, W. H., Pöschl, U.,
650 & Shiraiwa, M. (2018). Reactive oxygen species formed by secondary organic aerosols in water and
651 surrogate lung fluid. *Environmental Science & Technology*, *52*(20), 11642–11651.

652 Tositti, L, Brattich, E., Cinelli, G., & Baldacci, D. (2014). 12 years of 7Be and 210Pb in Mt. Cimone,
653 and their correlation with meteorological parameters. *Atmospheric Environment*, *87*, 108–122.
654 https://doi.org/https://doi.org/10.1016/j.atmosenv.2014.01.014

655 Tositti, Laura. (2017). The Relationship Between Health Effects and Airborne Particulate
656 Constituents. In *Clinical Handbook of Air Pollution-Related Diseases*. https://doi.org/10.1007/978-
657 3-319-62731-1_3

658 van den Berg, R., Hoefsloot, H., Westerhuis, J., Smilde, A., & van der Werf, M. (2006). Van den
659 Berg RA, Hoefsloot HCJ, Westerhuis JA, Smilde AK, Van der Werf MJ.. Centering, scaling, and
660 transformations: improving the biological information content of metabolomics data. BMC Genomics
661 7: 142-157. *BMC Genomics*, *7*, 142. https://doi.org/10.1186/1471-2164-7-142

662 Verma, V., Rico-Martínez, R., Kotra, N., King, L., Liu, J., Snell, T., & Weber, R. (2012). Contribution
663 of Water-Soluble and Insoluble Components and Their Hydrophobic/Hydrophilic Subfractions to the
664 Reactive Oxygen Species-Generating Potential of Fine Ambient Aerosols. *Environmental Science &*
665 *Technology*, *46*, 11384–11392. https://doi.org/10.1021/es302484r

666 Visentin, M., Pagnoni, A., Sarti, E., & Pietrogrande, M. C. (2016). Urban PM2. 5 oxidative potential:
667 Importance of chemical species and comparison of two spectrophotometric cell-free assays.
668 *Environmental Pollution*, *219*, 72–79.

669 Wissler, C. (1905). The Spearman Correlation Formula. *Science (New York, N.Y.)*, *22*, 309–311.
670 https://doi.org/10.1126/science.22.558.309

671 Xiong, Q., Yu, H., Wang, R., Wei, J., & Verma, V. (2017). Rethinking dithiothreitol-based particulate
672 matter oxidative potential: measuring dithiothreitol consumption versus reactive oxygen species
673 generation. *Environmental Science & Technology*, *51*(11), 6507–6514.

674 Yang, A., Jedyńska, A., Hellack, B., Kooter, I., Hoek, G., Brunekreef, B., Kuhlbusch, T. A. J., Cassee,
675 F., & Janssen, N. (2014). Measurement of the oxidative potential of PM2.5 and its constituents: The
676 effect of extraction solvent and filter type. *Atmospheric Environment*, *83*.
677 https://doi.org/10.1016/j.atmosenv.2013.10.049

Zhang, Y., Dai, M., & Yuan, Z. (2018). Methods for the detection of reactive oxygen species. *Analytical Methods*, *10*(38), 4625–4638.

Zhao, C.-N., Xu, Z., Wu, G.-C., Mao, Y.-M., Liu, L.-N., Dan, Y.-L., Tao, S.-S., Zhang, Q., Sam, N. B., & Fan, Y.-G. (2019). Emerging role of air pollution in autoimmune diseases. *Autoimmunity Reviews*.

FIGURES:

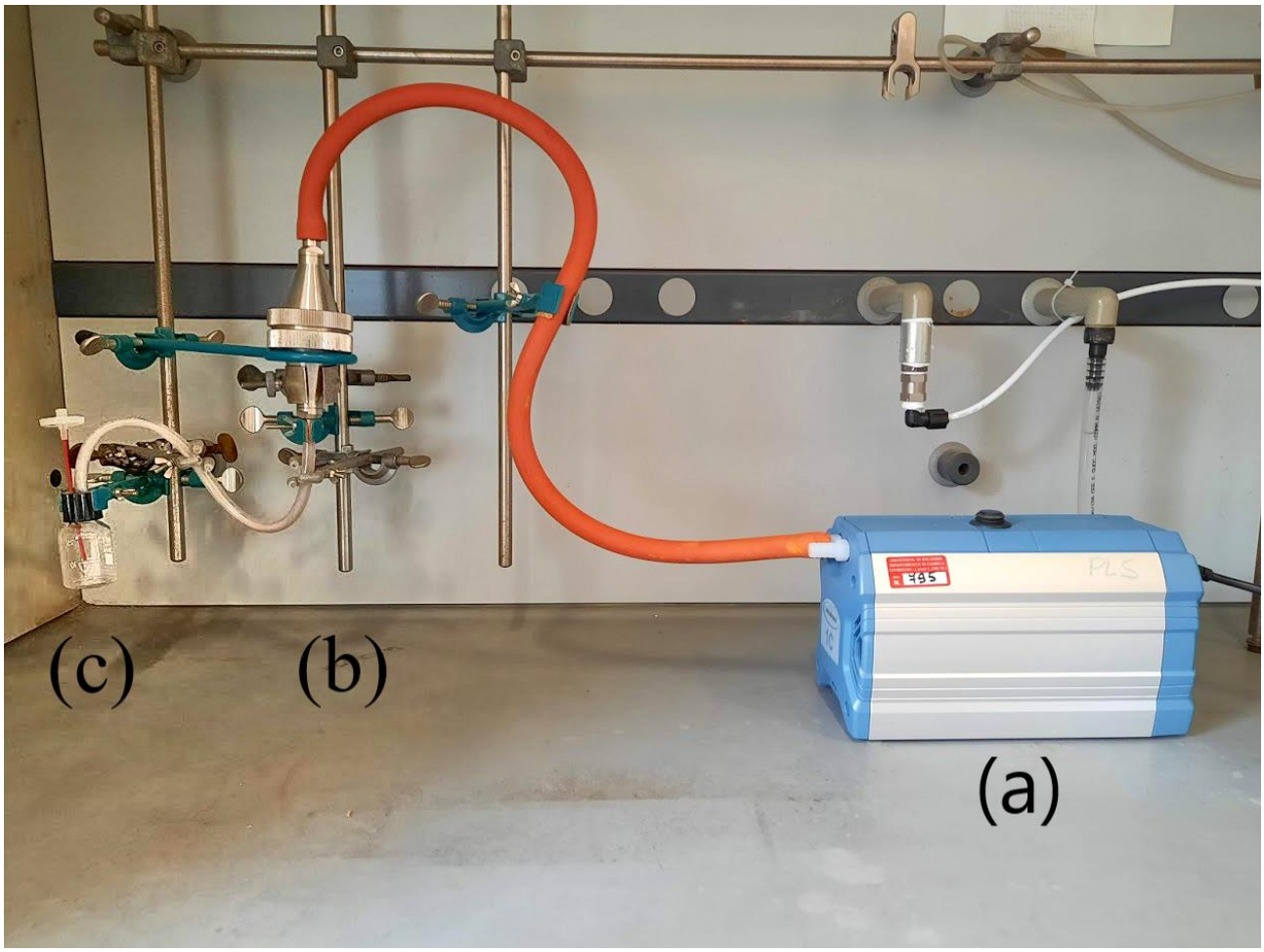

Figure 1. Assembled experimental set up of the resuspension chamber. From right to left: (a) Vacuubrand 1C pump (flow rate = 0.4/0.5 cfm), (b) 47 mm in-line filter holder, and (c) a resuspension chamber, a 25 ml Kitasato flask. The flask was modified by connecting the side-arm at a certain angle to the flask axis, in order to maximize the turbulence and the resulting resuspension of particles. During air suction, the flask was continuously kept under vibrational stirring to improve particulate homogeneity during the resuspension.

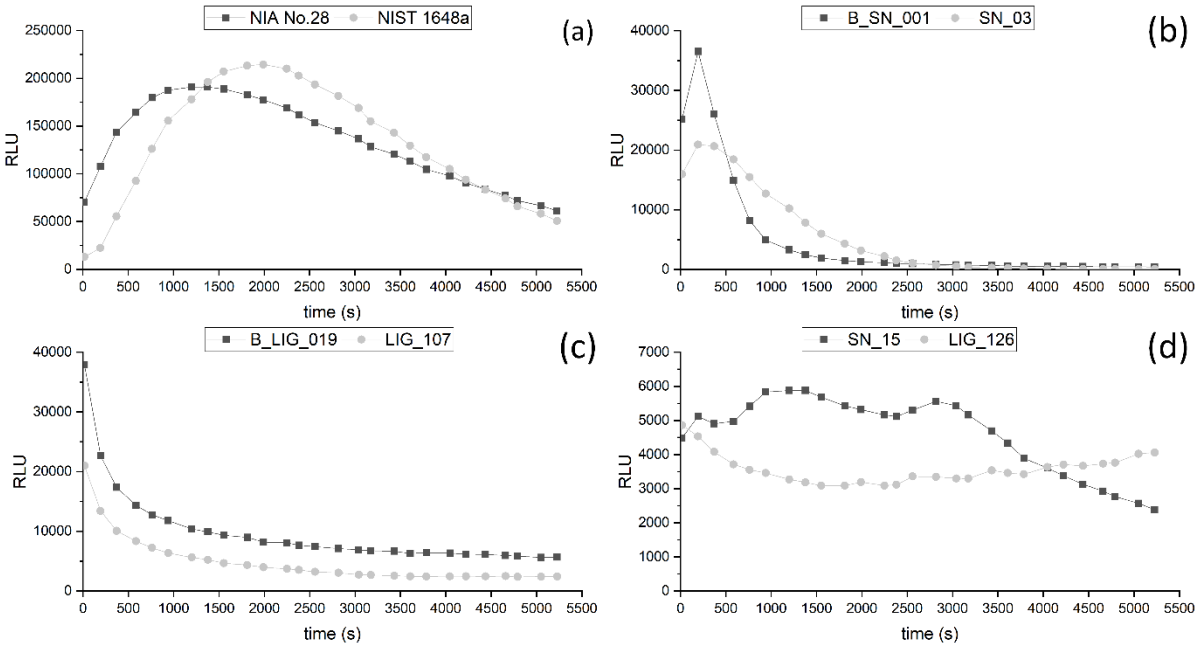

694

695 **Figure 2.** Light emission kinetics generated by luminol-based chemiluminescence analysis of
696 different particulate matter samples: a) the two certified standards, b) one Sierra Nevada (SN) sample
697 with its blank (B_SN) filter, c) one Ligurian (LIG) sample with its blank (B_LIG) filter, and d) two
698 peculiar samples.

699

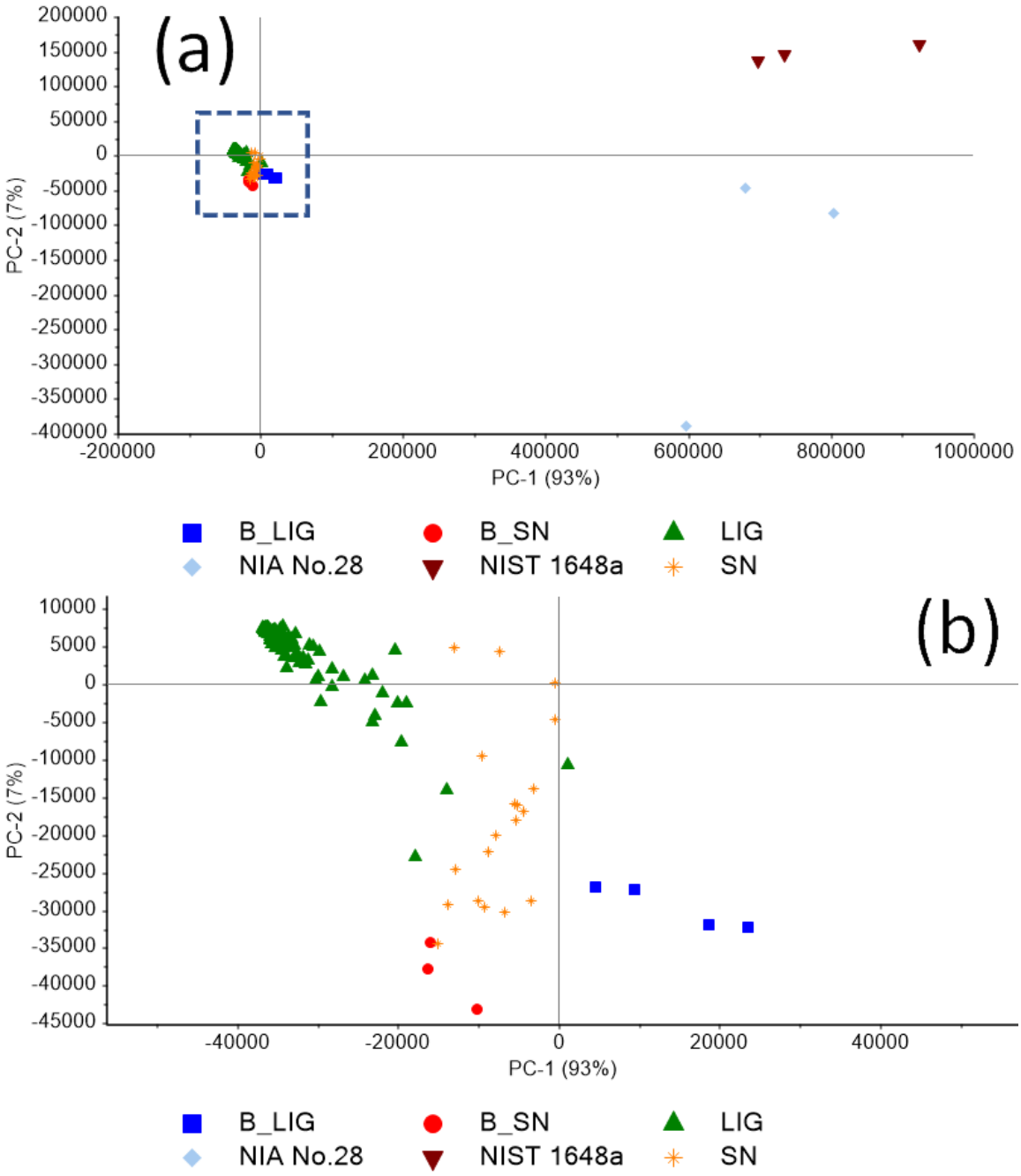

Figure 3. (a) Principal Component Analysis (PCA) scores plot including all the analyzed samples, PC-1 vs. PC-2. The graph portion inside the smaller dashed square is magnified into (b).

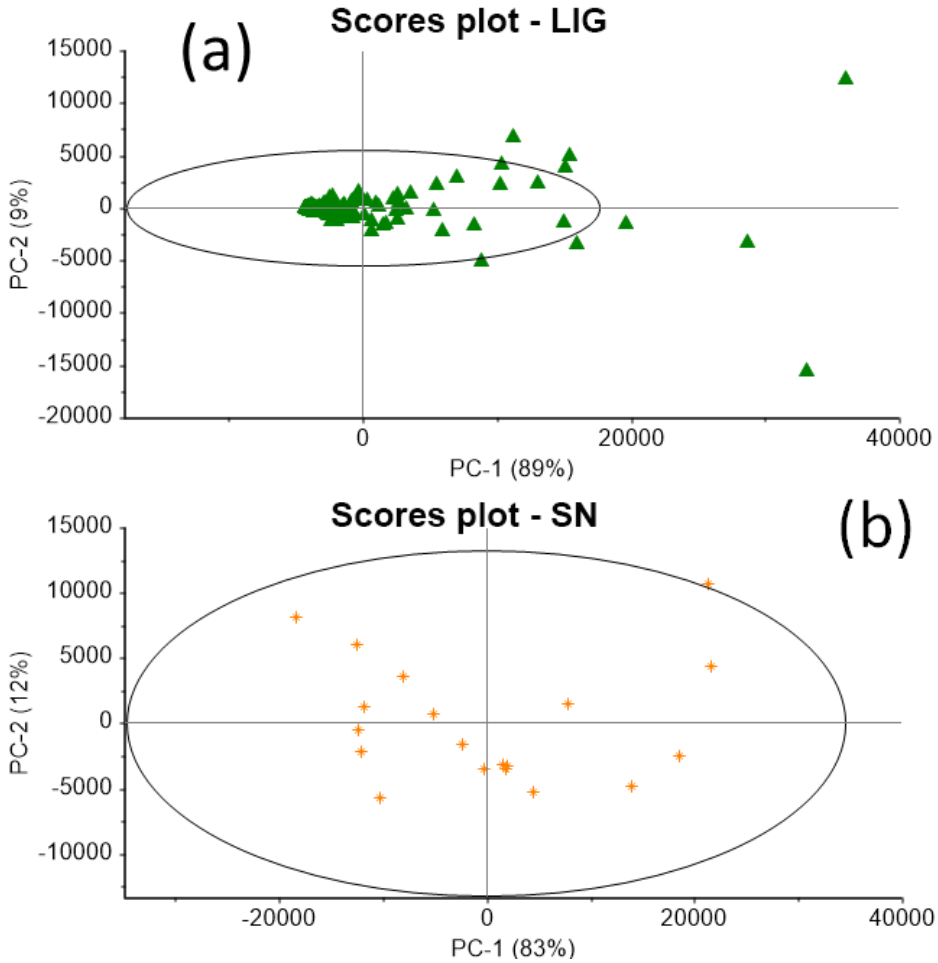

Figure 4. Scores plots of (a) LIG class-PCA (PC-1 vs. PC-2) and (b) SN class-PCA (PC-1 vs. PC-2).

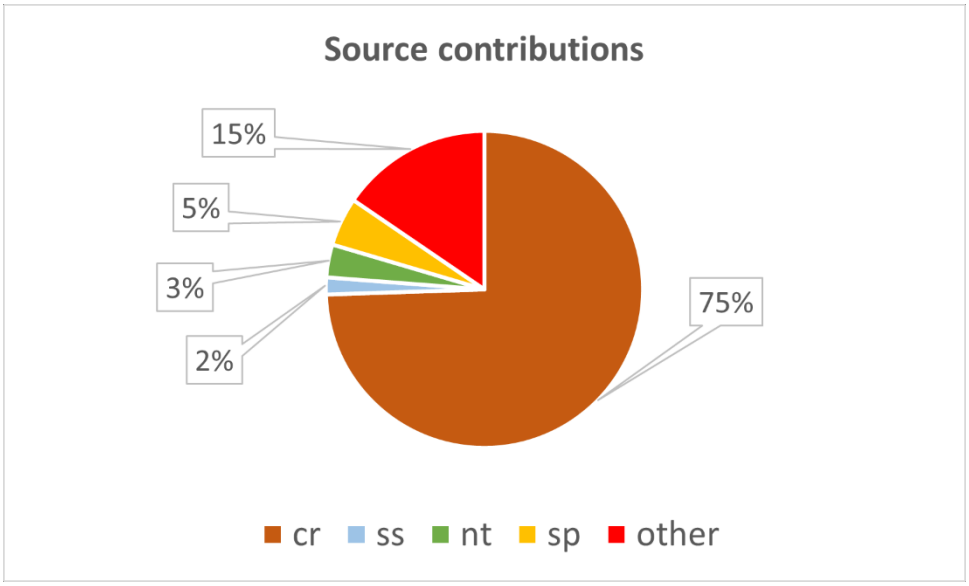

Figure 5. Source contributions (SN) of 17 - Soil Dust Composite Rural (cr), 157 - Aged sea spray (ss), 288 - Nitrate_PMF5 (nt), and 291 – Sulphate (sp) to PM_{10} mass. "Other" covers undetermined PM_{10} components.

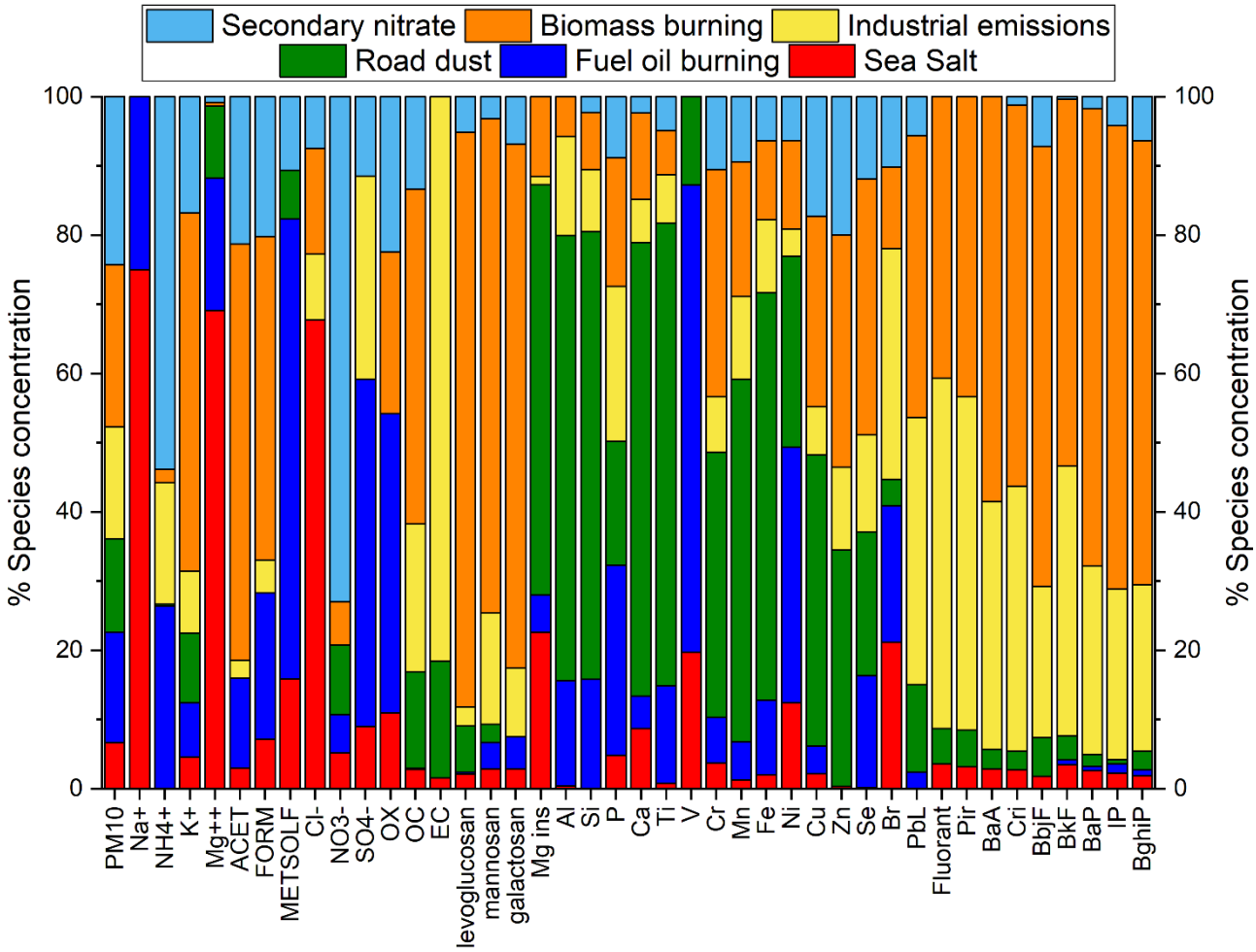

718

719 **Figure 6.** Source Fingerprints corresponding to the factors resolved by the PMF model (LIG).

720

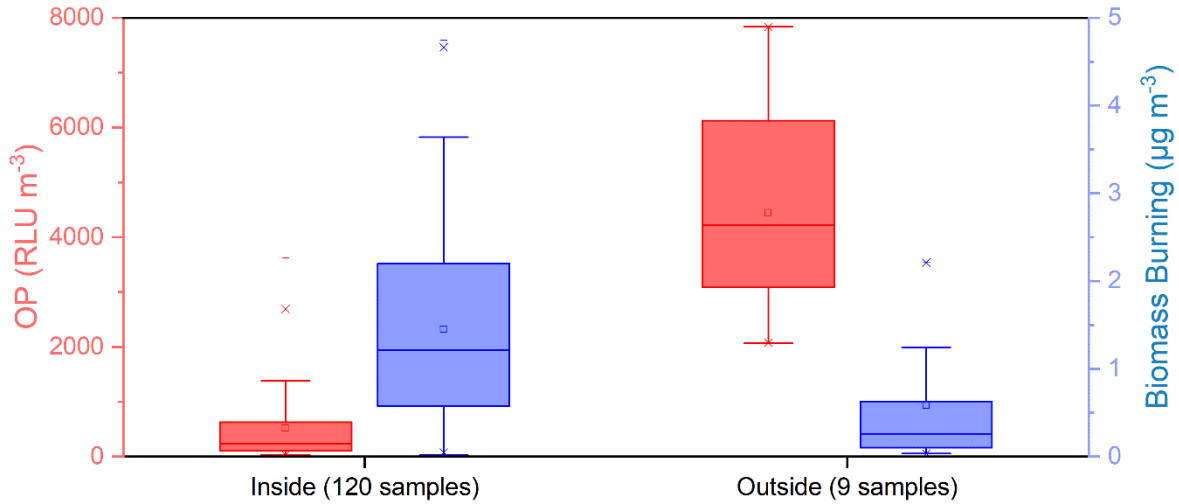

721

722 **Figure 7**. Comparison of the light intensity (OP) and the amount of Biomass Burning products
723 box chart graph between the Ligurian samples inside the 95%-Hotelling ellipse shown earlier in
724 Figure 4(a) (on the left) and outside the 95%-Hotelling ellipse (on the right).

TABLES:

Table 1. Spearman correlation coefficients (r_s) between the emission sources and the luminol-based oxidative potential (OP) for the Sierra Nevada (SN) and Ligurian (LIG) samples. The emission sources of these samples have already been described in paragraph 3.3. The most significant correlations ($|r_s| > 0.6$) have been marked with an asterisk.

(SN)		**(LIG)**	
emission source	**r_s OP**	**emission source**	**r_s OP**
Aged sea spray	+0.73*	Road dust	+0.23
Nitrate	+0.72*	Secondary Nitrate	+0.15
Sulphates	+0.72*	Fuel oil burning	+0.12
Soil dust Composite rural	+0.66*	Sea salt	-0.05
		Industrial emissions	-0.14
		Biomass Burning	-0.71*

CRediT author statement

Pietro Morozzi: Methodology, Formal analysis, Writing - Original Draft, Visualization

Luca Bolelli: Methodology, Investigation, Writing - Review & Editing

Erika Brattich: Writing - Review & Editing,

Elida Nora Ferri: Writing - Review & Editing,

Stefano Girotti: Conceptualization, Resources, Writing - Review & Editing, Supervision, Funding acquisition

Stefano Sangiorgi: Investigation, Writing - Review & Editing

J.A.G. Orza: Writing - Review & Editing,

Francisco Piñero-García: Supervision,

Laura Tositti: Conceptualization, Writing - Review & Editing, Supervision

Declaration of interests

☒ The authors declare that they have no known competing financial interests or personal relationships that could have appeared to influence the work reported in this paper.

☐The authors declare the following financial interests/personal relationships which may be considered as potential competing interests: